Silicon Raman polarizer

Victor V. Kozlov[1,2,*] and Stefan Wabnitz[1]

[1]*Department of Information Engineering, Università di Brescia, Via Branze 38, 25123 Brescia, Italy*

[2]*Department of Physics, St.-Petersburg State University, Petrodvoretz, St.-Petersburg 198504, Russia*

**Corresponding author: victor.kozlov@ing.unibs.it*

Received October 11, 2011; revised November 20, 2011; accepted January 2, 2012;
posted January 9, 2012 (Doc. ID 156315); published February 15, 2012

We theoretically investigate the polarization properties of Raman amplifiers based on silicon-on-insulator waveguides, and show that it is possible to realize a waveguide Raman polarizer. The Raman polarizer is a special type of Raman amplifier with the property of producing an amplified and highly repolarized beam when it is fed by a relatively weak and unpolarized signal. © 2012 Optical Society of America

OCIS codes: 230.5440, 230.1150, 230.4320.

Currently, the notion of Raman polarizers is associated with the effect of stimulated Raman scattering in silica fibers, following the pioneering experiments by Martinelli *et al.* using a span of telecom single-mode ultralow polarization mode dispersion (PMD) optical fiber [1]. It was shown that an initially unpolarized signal beam was transformed into a highly polarized beam at the fiber output. Such a polarizer works either in the co- or in the counter-propagating configuration [2–5]. The output signal state of polarization (SOP) is determined by the output or input SOP of the polarized pump beam. Fiber-based Raman polarizers are rather bulky and require ultralow-PMD fibers. Driven by the idea of miniaturization of this device, here we propose and design a silicon-based Raman polarizer.

Indeed, Raman gain in silicon is 10^4 times larger than in silica fiber. This enabled the experimental demonstration of efficient centimeter long silicon Raman amplifiers and lasers [6–10]. Moreover, the Raman response of silicon is highly anisotropic, [11,12] when the sample is pumped by a beam coupled to the TM mode. In this case the TE mode of the signal beam is maximally amplified, while the TM mode experiences virtually no amplification. It is this nonlinear anisotropy defined by the structure of the Raman tensor, which makes our Raman polarizer work. The TM-pump-induced Raman gain anisotropy stays in contrast with the usual TE-pumped configuration, where the Raman response is almost isotropic, hence not suitable for our purposes.

We choose to work with a rib-waveguide leak-free [13] geometry. This geometry has been proven the most suitable for the implementation of silicon Raman amplifiers and lasers [9,10], as it allows one to apply a bias and thereby suppress the nonlinear optical loss due to two-photon absorption (TPA)-induced free carrier absorption (FCA). Other geometries are also possible in principle, because the anisotropic Raman response that lies at the heart of the Raman polarizer is due to the material properties of silicon itself and not to waveguide anisotropy.

Let us consider a silicon-on-insulator (SOI) waveguide as shown in Fig. 1. In this geometry a strong pump beam is coupled to the TM mode of a 2 cm long waveguide along with a relatively weak Stokes signal seed with arbitrary SOP. In our simulations, we monitor the output power and SOP of the signal beam at the waveguide output. The input signal is weak enough to ensure an undepleted pump regime of Raman amplification along the entire sample. We repeated our numerical analysis for 10^4 different input signal SOPs, uniformly covering the Poincaré sphere, and study the resulting distribution of signal SOPs on the Poincare´ sphere at the output. The breadth of the SOP distribution is quantified in terms of the degree of polarization (DOP) (for its definition, see [3]). The Raman polarizer works properly when the output signal DOP is close to unity. This means that, on average, all input signal SOPs are attracted to the TE mode toward the waveguide output. As shown in Fig. 2, which summarizes the main result of the Letter, the DOP indeed stays close to unity, thereby indicating that our goal is reached.

The optical response of a SOI waveguide in the telecom band (in the vicinity of wavelength $\lambda = 1.55$ μm) is described well by equations given in [11]. Here we extend the scalar model of [11] to the vector case. Equations

$$\partial_y \phi_x = -(\alpha_s/2)\phi_x - [i\gamma_s + (\beta_s/2)][P_x^{\mathrm{SPM}}(\omega_s) + 2P_x^{\mathrm{XPM}}(\omega_s)] + (g_s/2)P_x^{R}(\omega_s) - (\xi_s/2)P_x^{\mathrm{FCA}}(\omega_s), \quad (1)$$

$$\partial_y \phi_z = -(\alpha_s/2)\phi_z - [i\gamma_s + (\beta_s/2)][P_z^{\mathrm{SPM}}(\omega_s) + 2P_z^{\mathrm{XPM}}(\omega_s)] + (g_s/2)P_z^{\mathrm{R}}(\omega_s) - (\xi_s/2)P_z^{\mathrm{FCA}}(\omega_s) \quad (2)$$

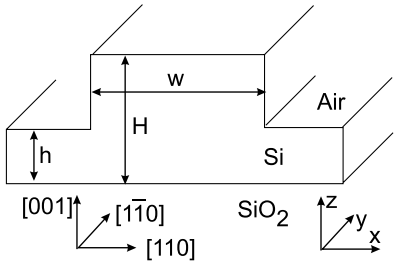

Fig. 1. Rib-waveguide geometry [7]. Parameters are width w, slab height h, and rib height H, with ratios $w/h = 2/1.4$ and $w/H = 2/2.15$. We take $w = 1.2$; 0.8 (μm). However, waveguides with $w = 0.4$ μm are not leak-proof.

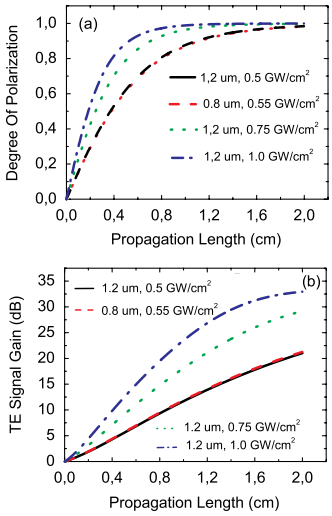

Fig. 2. (Color online) (a) DOP and (b) gain of the signal beam, both as a function of the propagation length for different waveguide widths and pump intensities. Parameters are $\lambda_s = 1.55\ \mu$m, $\lambda_s = 1.434\ \mu$m, $\alpha_{s,p} = 0.25\ \text{cm}^{-1}$, $\gamma_{s,p} = 2.4\ \text{cm/GW}$, $\beta_{s,p} = 0.5\ \text{cm/GW}$, $g_s = (\omega_s/\omega_p)g_p = 20\ \text{cm/GW}$, $\xi_s = (\omega_s/\omega_p)^2\xi_p = 4.5\ \text{cm}^3/\text{GW}^2$.

are formulated for two orthogonal polarization components of the signal field $\phi_{x,z}$ centered at frequency ω_s and normalized such that $|\phi_{x,z}|^2$ is the intensity measured in units of GW/cm^2. Similar equations with indices s and p interchanged hold for the polarization components of the pump beam $\psi_{x,z}$ centered at frequency ω_p. Here the strength of the Kerr response is described by the nonlinear coefficients $\gamma_{s,p}$, the Raman response is described by $g_{p,s}$, the TPA coefficients are $\beta_{s,p}$, the FCA coefficients are $\xi_{p,s}$, and finally linear losses are characterized by the absorption coefficients $\alpha_{s,p}$. We also assume that the quasi-TE mode is polarized along the x direction and the quasi-TM mode along the z direction, while the signal and pump beams copropagate along the y direction. The polarization sources $P^{\text{SPM}}_{x,z}(\omega_{s,p})$, $P^{\text{XPM}}_{x,z}(\omega_{s,p})$, and $P^{R}_{x,z}(\omega_{s,p})$ describe the cubic response of the silicon produced by the self- and cross-interaction of two intense beams. Self-phase modulation (SPM) term $P^{SPM}_x(\omega_s)$ contains the three terms

$$P^{\text{SPM}}_x = R^e_{ijkl}[A^{xxxx}_{ijkl}|\phi_x|^2 + (A^{xzzx}_{ijkl} + A^{xxzz}_{ijkl})|\phi_z|^2]\phi_x, \quad (3)$$

where $i,j,k,l = x,z$, and the summation is assumed over repeated lower indices. By interchanging indices x and z, we get from Eq. (3) the expression for $P^{\text{SPM}}_z(\omega_s)$. Note that in writing down Eq. (3) we ignored five additional terms, because they contain the fast oscillating exponential $\exp\{i[\beta_z(\omega_s) - \beta_x(\omega_s)]y\}$, where $\beta_x(\omega_s)$ and $\beta_z(\omega_s)$ are the wave numbers for the TE and TM modes, respectively. For the waveguide geometry shown in Fig. 1 $[\beta_x(\omega_s) - \beta_z(\omega_s)] \sim 400\ \text{cm}^{-1}$ for $w = 1.2\ \mu$m, and it gets even larger for submicrometer (e.g., $w = 0.8\ \mu$m) waveguides. Over a length of 2 cm all terms containing this exponential are quickly averaged to zero. Similar considerations lead us to the spatially averaged expression of the cross-phase modulation (XPM) term

$$P^{\text{XPM}}_x(\omega_s) = R^e_{ijkl}[B^{xxxx}_{ijkl}|\psi_x|^2 + B^{xzzx}_{ijkl}|\psi_z|^2]\phi_x. \quad (4)$$

In writing down Eq. (4) the terms containing exponential $\exp(i\{[\beta_z(\omega_s) - \beta_x(\omega_s)] - [\beta_z(\omega_p) - \beta_x(\omega_p)]\}y)$ were also ignored as they are fast rotating. For the Raman-induced polarization, the expression looks very similar:

$$P^{R}_x(\omega_s) = R^R_{ijkl}[B^{xxxx}_{ijkl}|\psi_x|^2 + B^{xzzx}_{ijkl}|\psi_z|^2]\phi_x, \quad (5)$$

with the only change that the Kerr tensor R^e_{ijkl} was substituted by the Raman tensor R^R_{ijkl}. Finally, the FCA polarization reads

$$P^{\text{FCA}}_x(\omega_s) = [D^{ssssss}_{xjjkkx}|\phi_j|^2|\phi_k|^2 + D^{sppsss}_{xjjkkx}|\psi_j|^2|\phi_k|^2 + D^{spppps}_{xjjkkx}|\psi_j|^2|\psi_k|^2 + D^{ssspps}_{xjjkkx}|\phi_j|^2|\psi_k|^2]\phi_x. \quad (6)$$

Coefficients A, B, and D stand for overlap of modes denoted here as F. These overlap integrals are:

$$A^{\alpha\beta\gamma\sigma}_{ijkl} = \frac{\sqrt{n_\alpha n_\beta n_\gamma n_\sigma}}{n_\alpha^2}\left\{\iint \text{d}x\text{d}z|F^\alpha_i(\omega_s)|^2\right\}^{-1} \times \iint dxdz[F^\alpha_i(\omega_s)]^* F^\beta_j(\omega_s)[F^\gamma_k(\omega_s)]^* F^\sigma_l(\omega_s), \quad (7)$$

$$B^{\alpha\beta\gamma\sigma}_{ijkl} = \frac{\sqrt{n_\alpha n_\beta n_\gamma n_\sigma}}{n_\alpha^2}\left\{\iint \text{d}x\text{d}z|F^\alpha_i(\omega_s)|^2\right\}^{-1} \times \iint \text{d}x\text{d}z[F^\alpha_i(\omega_s)]^* F^\beta_j(\omega_p)[F^\gamma_k(\omega_p)]^* F^\sigma_l(\omega_s), \quad (8)$$

where $\alpha,\beta,\gamma,\sigma = x,z$ and n_α is the effective index of the mode, and

$$D^{\alpha\beta\beta\gamma\gamma\alpha}_{ijjkki} = \frac{n_i n_j n_k}{n_i^3}\left\{\iint \text{d}x\text{d}z|F_i(\omega_\alpha)|^2\right\}^{-1} \times \iint \text{d}x\text{d}z|F_i(\omega_\alpha)|^2|F_j(\omega_\beta)|^2|F_k(\omega_\gamma)|^2, \quad (9)$$

where $\alpha,\beta,\gamma,\sigma = s,p$. Finally, we need to define the tensorial nonlinear optical response of silicon. Thus, the Kerr and Raman tensors are [7,11]

$$R^e_{ijkl} = (\rho/3)(\delta_{ij}\delta_{kl} + \delta_{ik}\delta_{jl} + \delta_{il}\delta_{jk}) + (1-\rho)\sum_{s=1}^{3} M_{si}M_{sj}M_{sk}M_{sl}, \quad (10)$$

$$R^R_{ijkl} = \delta_{ik}\delta_{jl} + \delta_{il}\delta_{jk} - 2\sum_{s=1}^{3} M_{si}M_{sj}M_{sk}M_{sl}, \quad (11)$$

where δ is Kronecker's symbol, M is a 3×3 matrix with $M_{11} = 1$, $M_{22} = M_{32} = M_{33} = -M_{23} = 2^{-1/2}$, which are the only nonzero elements, and $\rho = 1.27$ in the telecom band. In Table 1 we report the overlap coefficients of the waveguide modes at ω_s for two different geometries,

Table 1. Nonlinear Coupling Coefficients at ω_s for a Rib Waveguide Shown in Fig. 1, for Two Rib Widths

$w(\mu\text{m})$	$R^e_{ijkl}A^{xxxx}_{ijkl}$	$R^e_{ijkl}A^{xzzx}_{ijkl}$	$R^e_{ijkl}A^{zzzz}_{ijkl}$	$R^e_{ijkl}A^{zxxz}_{ijkl}$	$R^e_{ijkl}B^{xxxx}_{ijkl}$	$R^e_{ijkl}B^{xzzx}_{ijkl}$	D^{ssssss}_{xxxxxx}
1.2	0.5830	0.1990	0.5416	0.2495	0.5795	0.1990	0.3468
0.8	0.5697	0.1897	0.5558	0.2726	0.5633	0.1860	0.3343
$w(\mu\text{m})$	$R^e_{ijkl}B^{zzzz}_{ijkl}$	$R^e_{ijkl}B^{zxxz}_{ijkl}$	$R^R_{ijkl}B^{xxxx}_{ijkl}$	$R^R_{ijkl}B^{xzzx}_{ijkl}$	$R^R_{ijkl}B^{zzzz}_{ijkl}$	$R^R_{ijkl}B^{zxxz}_{ijkl}$	D^{spppps}_{xzzzzx}
1.2	0.5424	0.2483	0.5060	0.4652	0.0021	0.5796	0.3066
0.8	0.5535	0.2700	0.4880	0.4247	0.0145	0.6090	0.2725

in order to show how the anisotropies of the Kerr and Raman response are modified when the waveguide dimensions are reduced below $1\,\mu$m. The overlap coefficients for the pump beam (not shown here) differ only slightly (<20%) from signal coefficients. Note that in the undepleted pump regime, the only relevant D coefficients are D^{spppps}_{xzzzzx} and D^{pppppp}_{zzzzzz}.

The results of Fig. 2 demonstrate that indeed it is possible to implement an efficient silicon waveguide-based Raman polarizer. Indeed, Fig. 2 shows that a signal DOP very close to unity is obtained whenever the pump intensity leads to Raman gains of 20 dB or larger. In Fig. 2 we also show that if the waveguide width is reduced from $w = 1.2\ \mu$m to $w = 0.8\ \mu$m, the pump intensity should be increased by 10% for maintaining the same Raman gain and DOP for the signal, owing to the reduced corresponding overlap coefficient (see Table 1) in this case.

In conclusion we proposed the silicon TM-pumped Raman polarizer, and numerically verified its performance in the telecom band. In particular, we have shown that an initially weak and arbitrarily polarized signal beam is transformed into an amplified beam coupled to the waveguide TE mode. The principle of operation of the silicon polarizer is not limited to the undepleted pump regime only: the polarizer may also operate in the depleted regime. Our scheme can be extended to the mid-IR, where TPA and FCA effects are no longer relevant. Also, the cw configuration that was considered here can be extended to the regime of pulsed excitation, where FCA effects are not as detrimental as in the cw case. Whenever the gain of a single Raman polarizer is not high enough, one may think of a cascaded Raman polarizer—for instance, two sequential polarizers with 10 dB gain can perform nearly as well as one Raman polarizer of 20 dB gain. The nominal bandwidth of the Raman polarizer is 106 GHz (compare to ≈5 THz in silica fibers), which is the width of the Raman peak in silicon. This bandwidth can be broadened by using multiple pumps, thus allowing for WDM operation.

The specific waveguides proposed in this Letter are free from TM-mode lateral leakage loss [13]. For leaky waveguides (e.g., for $w = 0.4\ \mu$m), one may also obtain an efficient Raman polarizer with a pump coupled to the TE mode. In this case, it is not the nonlinear Raman anisotropy that provides a discrimination between the preferentially amplified signal TE mode and the unamplified signal TM mode, but rather the loss anisotropy between the two signal polarization components.

Among the potential applications of silicon Raman polarizers are: (i) active on-chip polarizers, that not only repolarize light, but also compensate for propagation and interconnection losses, e.g., compact preamplifiers and simultaneously polarizers at the receiver end of an optical communication line for further polarization-sensitive (nonlinear) optical postprocessing; (ii) silicon Raman lasers with a well defined SOP.

We thank Daniele Modotto for numerous valuable discussions. This work was carried out with support from the Programma di Ricerca Scientifica di Rilevante Interesse Nazionale project “Nonlinear cross-polarization interactions in photonic devices and systems,” and from the Fondazione Cariplo grant No. 2009-2730.

References

1. M. Martinelli, M. Cirigliano, M. Ferrario, L. Marazzi, and P. Martelli, Opt. Express **17**, 947 (2009).
2. V. V. Kozlov, J. Nuño, J. D. Ania-Castañón, and S. Wabnitz, Opt. Lett. **35**, 3970 (2010).
3. V. V. Kozlov, J. Nuño, J. D. Ania-Castañón, and S. Wabnitz, J. Lightwave Technol. **29**, 341 (2011).
4. L. Ursini, M. Santagiustina, and L. Palmieri, IEEE Photon. Technol. Lett. **23**, 254 (2011).
5. F. Chiarello, L. Ursini, L. Palmieri, and M. Santagiustina, IEEE Photon. Technol. Lett. **23**, 1457 (2011).
6. R. Claps, D. Dimitropoulus, Y. Han, and B. Jalali, Opt. Express **10**, 1305 (2002).
7. D. Dimitropoulos, B. Houshmand, R. Claps, and B. Jalali, Opt. Lett. **28**, 1954 (2003).
8. V. Raghunathan, D. Borlaug, R. R. Rice, and B. Jalali, Opt. Express **15**, 14355 (2007).
9. H. Rong, R. Jones, A. Liu, O. Cohen, D. Hak, A. Fang, and M. Paniccia, Nature **433**, 725 (2005).
10. H. Rong, A. Liu, R. Jones, O. Cohen, D. Hak, R. Nicolaescu, A. Fang, and M. Paniccia, Nature **433**, 292 (2005).
11. Q. Lin, O. J. Painter, and G. P. Agrawal, Opt. Express **15**, 16604 (2007).
12. T. K. Liang and H. K. Tsang, in *1st IEEE International Conference on Group IV Photonics* (IEEE, 2004), paper WA4.
13. M. A. Webster, R. M. Pafchek, A. Mitchell, and T. L. Koch, IEEE Photon. Technol. Lett. **19**, 429 (2007).